

likely to be a transition state rather than a stable structure. This prediction is at variance with the conclusions drawn by Nakamura et al.²²

The curve-crossing model thus unifies the hypercoordination problem with the delocalization¹³ and reactivity problems.¹⁰⁻¹³ On the basis of elementary thermochemistry, it is possible to pattern the trends in the stability of hypercoordinated, delocalized, and transition-state species relative to their normal-valent constituents.

Extension to other hypercoordinated radicals is in progress.

Acknowledgment. We are grateful to Dr. J. Roncin for helpful discussions and to Dr. E. Evleth for communicating his results to us prior to publication. S.S.S. thanks the Université de Paris-Sud for a Visiting Professorship, during which time this paper was shaped. We thank the scientific committee of the CCVR for a grant (ATP 3872) on the Cray-1S computer (Palaiseau).

Theoretical Study of the Electronic Structures and Absorption Spectra of $\text{Pt}(\text{CN})_4^{2-}$ and $\text{Tl}_2\text{Pt}(\text{CN})_4$ Based on Density Functional Theory Including Relativistic Effects

Tom Ziegler,^{*,†} Jeffrey K. Nagle,^{*,‡} Jaap G. Snijders,[§] and Evert J. Baerends[§]

Contribution from the Department of Chemistry, University of Calgary, Calgary, Alberta, Canada T2N 1N4, Department of Chemistry, Bowdoin College, Brunswick, Maine 04011, and Department of Theoretical Chemistry, Free University, De Boelelaan 1083, 1081 HV Amsterdam, The Netherlands. Received August 22, 1988

Abstract: Density functional calculations on $\text{Pt}(\text{CN})_4^{2-}$ (**1**) and the recently reported $\text{Tl}_2\text{Pt}(\text{CN})_4$ (**2**) have been carried out in both the nonrelativistic and quasi-relativistic limits. This has led to a new and detailed understanding of the electronic structure of **1**. Electronic transition energies for **1** have been calculated from state function energy differences to help clarify many of the spectroscopic properties of this ion. This is the first time such calculations have been performed using density functional theory. The interaction between **1** and Tl^+ ions in **2** is shown to be largely ionic in nature but with a substantial covalent component (189 kJ mol⁻¹). It is suggested that the Tl^+ ions in **2** provide a spectroscopic probe that could enable a rigorous comparison to be made between electronic structure calculations and polarized single-crystal absorption and emission spectra.

The bonding and spectroscopy of $\text{Pt}(\text{CN})_4^{2-}$ (**1**) continue to attract attention.¹ As an isolated ion it serves as a model for understanding the bonding and spectroscopic properties of d⁸ square-planar compounds possessing strong field ligands. Perhaps even greater interest centers on the ability of **1** to form columnar structures in the solid state with adjacent Pt atoms separated by 310–370 pm.² Such stacking results in the appearance of a low-energy absorption band often accompanied by a corresponding visible luminescence.¹

Despite many attempts over the years, both experimental and theoretical, some issues regarding the bonding and spectroscopic properties of **1** remain unresolved.¹ Perhaps the greatest uncertainty concerns the relative energy ordering of the Pt 5d orbitals and its effect on the spectroscopic properties of the ion. This ordering has important implications also for establishing the mechanism by which the ions stack to form columnar structures.

Although more than 20 different columnar compounds containing **1** and various metal ions are known,² the recently reported structure of $\text{Tl}_2\text{Pt}(\text{CN})_4$ (**2**) reveals it to be unique in that it is not columnar but consists of discrete octahedral molecules with Pt–Tl bonds.³ As such it serves as perhaps the simplest example of a growing class of structurally characterized compounds found to possess relatively short internuclear distances between d-block elements like Ir, Pt, and Au and p-block elements like Tl and Pb.⁴ Evidence has been obtained for the presence of covalent metal-metal interactions in these⁴ and related but structurally uncharacterized compounds.⁵ The recent report of a strongly luminescent exciplex formed between $\text{Pt}_2(\text{P}_2\text{O}_5\text{H}_2)_4^{4-}$ and Tl^+ in aqueous solution is also of interest in this context.⁶ It is therefore of some importance to determine the nature of the bonding in **2**

to see if any useful generalizations can be made about the bonding in this group of compounds.

One of the best ways to understand the bonding and spectroscopy in **1** and **2** is to do reliable electronic structure calculations. Reported here are the results of density functional calculations on **1** and **2**. Relativistic effects have been taken into account due to the presence of the heavy Pt and Tl atoms. Detailed spectroscopic assignments based on the inclusion of spin-orbit coupling are possible using this approach and enable a comparison with the well-studied spectrum of **1** to be made. This is the first relativistic density functional calculation on the electronic spectrum

(1) For recent reviews and pertinent references, see: Gliemann, G.; Yersin, H. *Struct. Bonding* **1985**, *62*, 89–153. Hoffmann, R. *Angew. Chem., Int. Ed. Engl.* **1987**, *26*, 846–878.

(2) Williams, J. M. *Adv. Inorg. Chem. Radiochem.* **1983**, *26*, 235–268.

(3) Nagle, J. K.; Balch, A. L.; Olmstead, M. M. *J. Am. Chem. Soc.* **1988**, *110*, 319–321.

(4) (a) $\text{Ir}_2\text{M}(\text{CO})_2\text{Cl}_2\{\mu\text{-}[(\text{C}_6\text{H}_5)_2\text{PCH}_2]_2\text{As}(\text{C}_6\text{H}_5)_2\}_2^+$ (M = Tl, Pb): Balch, A. L.; Nagle, J. K.; Olmstead, M. M.; Reedy, P. E., Jr. *J. Am. Chem. Soc.* **1987**, *109*, 4123–4124. (b) $\text{Tl}[\text{Au}(\text{CN})_2]$: Blom, N.; Ludi, A.; Bürgi, H.-B.; Tlchy, K. *Acta Crystallogr., Sect. C: Cryst. Struct. Commun.* **1984**, *C40*, 1767–1769. (c) $\text{Pt}[\text{P}(\text{C}_6\text{H}_5)_3]_2[\text{Pb}(\text{C}_6\text{H}_5)_2]$: Crocinal, B.; Nicolini, M.; Clemente, D. A.; Bandoni, G. *J. Organomet. Chem.* **1973**, *49*, 249–256. (d) $\text{AuTl}[(\text{C}_6\text{H}_5)_2\text{P}(\text{CH}_2\text{S})_2]$: Wang, S.; Fackler, J. P., Jr.; King, C.; Wang, J. C. *J. Am. Chem. Soc.* **1988**, *110*, 3308–3310. (e) $\text{Au}_2\text{Pb}[(\text{C}_6\text{H}_5)_2\text{P}(\text{CH}_2\text{S})_2]$: Wang, S.; Garzon, G.; Wang, J. C.; Fackler, J. P., Jr., unpublished results. (f) $\text{TlPt}_3(\text{CO})_3[\text{P}(\text{C}_6\text{H}_{11})_3]_3^+$: Ezomo, O. J.; Mingos, D. M. P.; Williams, I. D. *J. Chem. Soc., Chem. Commun.* **1987**, 924–925.

(5) (a) $\text{PtL}_2[\text{Pb}(\text{C}_6\text{H}_5)_3]_2$ [L = $\text{P}(\text{C}_2\text{H}_5)_3$, $\text{As}(\text{C}_2\text{H}_5)_3$]: Deganello, G.; Carturan, G.; Belluco, U. *J. Chem. Soc. A* **1968**, 2873–2878. (b) $\text{Pt}[\text{P}(\text{C}_6\text{H}_5)_3]_2(\text{Br})(\text{C}_6\text{H}_5)[\text{Ti}(\text{C}_6\text{F}_5)\text{Br}]$: Nyholm, R. S. *Q. Rev.* **1970**, *24*, 1–19. (c) $\text{Ir}(\text{CO})(\text{O}_2\text{CR})\text{L}_2\text{X}[\text{Ti}(\text{O}_2\text{CR})_2]$ (R = CH_3 , C_2H_5 , $\text{CH}(\text{CH}_3)_2$, CF_3 , L = $\text{P}(\text{C}_6\text{H}_5)_3$, $\text{P}(\text{CH}_3)_2\text{C}_6\text{H}_5$, $\text{As}(\text{C}_6\text{H}_5)_3$; X = Cl, O_2CR): Van Vliet, P. I.; Vrleze, K. *J. Organomet. Chem.* **1977**, *139*, 337–347. (d) $[\text{Ir}(\text{bta})_2[\text{P}(\text{C}_6\text{H}_5)_3\text{Tl}]\text{C}_6\text{H}_6$ (bta = benzotriazenido): Brown, L. D.; Ibers, J. A.; Siedle, A. R. *Inorg. Chem.* **1978**, *17*, 3026–3030.

(6) Nagle, J. K.; Brennan, B. A. *J. Am. Chem. Soc.* **1988**, *110*, 5931–5932.

[†] University of Calgary.

[‡] Bowdoin College.

[§] Free University.

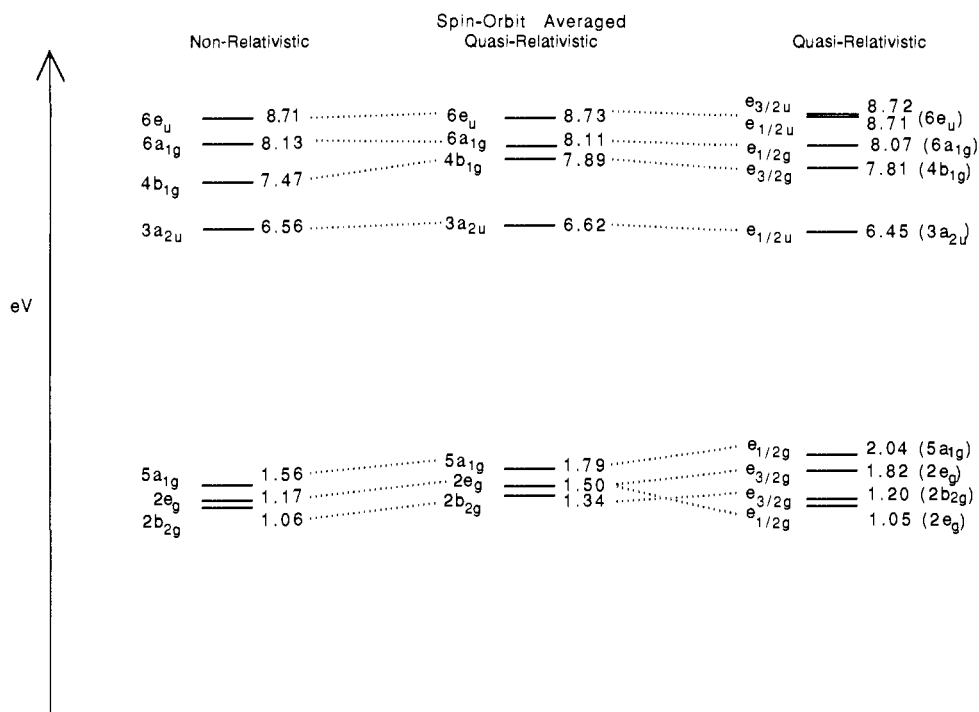


Figure 1. Orbital energy diagram (all values in electronvolts) showing the effects of relativity on the ordering of the Pt 5d-based orbitals in $\text{Pt}(\text{CN})_4^{2-}$. The spin-orbit averaged quasi-relativistic results include all relativistic effects except spin-orbit coupling.

of a compound in which the excitation energies are calculated in a proper way from state functions rather than just simple one-electron energy differences. Two relativistic calculations of **1** have been reported.^{7,8} There have been no previous theoretical studies of **2**.

Computational Details

All calculations were based on the LCAO-HFS program system due to Baerends et al.⁹ or its relativistic extension due to Snijders et al.¹⁰ The density functional employed was that of the Hartree-Fock-Slater method¹¹ augmented by Becke's¹² nonlocal exchange correction as well as Gunnarsson and Lundquist's local spin density functional for the correlation,¹³ including Stoll's correction for self-interaction¹⁴ based on Vosko's¹⁵ parametrization from electron gas data. The exchange parameter α_{ex} was given the electron gas value of $2/3$.

An uncontracted triple- ζ STO basis set¹⁶ was employed for the 5s, 5p, 5d, 6s, and 6p orbitals of Pt and Tl, whereas the 2s and 2p orbitals of C and N were represented by a double- ζ STO basis set augmented by a single 3d-STO. The other shells of lower energy were considered as core and frozen according to the method of Baerends et al.⁹ To describe accurately the Coulomb and exchange potentials, extensive fits¹⁷ of the density were carried out using a set of fit functions including s-, p-, d-,

f-, and g-type functions. The structural parameters for $\text{Pt}(\text{CN})_4^{2-}$ and $\text{Tl}_2\text{Pt}(\text{CN})_4$ were taken from ref 3.

The influence of relativity is introduced in two stages. In the first stage all first-order relativistic corrections, except for spin-orbit coupling, are included in a spin-orbit averaged quasi-relativistic calculation.¹⁰ The introduction in the second step of spin-orbit coupling requires a relabeling of the d-based orbitals according to double group symmetry. Thus 5a_{1g} and one component of 2e_g transform as e_{1/2g} according to D_{4h}' (the prime indicates double group representations) whereas 2b_g and the other component of 2e_g transform as e_{3/2g}.

The nonrelativistic and spin-orbit averaged quasi-relativistic excitation energies were calculated by using the generalized transition-state method¹⁸ and a procedure given elsewhere¹⁹ for evaluating singlet-triplet splittings. The spin-orbit splittings were calculated by transforming functions representing the ground and excited states from the spin-orbit averaged quasi-relativistic calculations (by a unitary transformation using the tables given by Koster et al.²⁰) to a basis spanning the D_{4h}' double group. The spin-orbit interactions between states of the same D_{4h}' double group symmetry were subsequently evaluated and the resulting matrix elements calculated by using an established method.¹⁰

In both the nonrelativistic and spin-orbit averaged quasi-relativistic calculations (all relativistic effects but spin-orbit coupling included) the states are listed by using single group symmetry labels and so retain the singlet or triplet spin designation. In the quasi-relativistic calculation, which includes spin-orbit coupling, the states are listed by using double group symmetry labels indicated by primes.

Results and Discussion

1. $\text{Pt}(\text{CN})_4^{2-}$: Electronic Structure Calculations. Application of the simple crystal field²¹ or angular overlap²² model predicts the ordering of the energies of the 5d orbitals (from highest to lowest) to be $d_{x^2-y^2} \gg d_{z^2} > d_{xy} > d_{xz}, d_{yz}$. Aside from the reversal of the d_{xy} and d_{xz}, d_{yz} levels (due to extensive mixing of the Pt 5d_{xz,yz} and 5d_{xy} orbitals with the CN⁻ π orbitals), this is the same ordering found from the density functional calculations in both the non-relativistic and quasi-relativistic limits as shown in Figure 1. With

(18) Ziegler, T.; Rauk, A. *Theor. Chim. Acta* **1977**, *46*, 1-10.

(19) Ziegler, T.; Rauk, A.; Baerends, E. J. *Theor. Chim. Acta* **1977**, *43*, 261-271.

(20) Koster, G. F.; Dimmock, J. O.; Wheeler, R. G.; Statz, H. In *Properties of the Thirty-Two Point Groups*; MIT Press: Cambridge, MA, 1963.

(21) Burdett, J. K. *Molecular Shapes*; Wiley: New York, 1980; p 138. See also: Albright, T.; Burdett, J. K.; Whangbo, M. H. *Orbital Interactions in Chemistry*; Wiley: New York, 1985.

(22) Reference 21, p 148.

(7) Lopez, J. P.; Yang, C. Y.; Case, D. A. *Chem. Phys. Lett.* **1982**, *91*, 353-357. Yang, C. Y.; Case, D. A. In *Local Density Approximations in Quantum Chemistry and Solid State Physics*; Dahl, J. P., Avery, J., Eds.; Plenum Press: New York, 1984; pp 643-664. Yang, C. Y. In *Relativistic Effects in Atoms, Molecules, and Solids*; Malli, G. L., Ed.; NATO ASI Ser. B, Phys., Plenum Press: New York, 1983; Vol. 29, pp 335-361.

(8) Carsey, T. P.; Boudreaux, E. A. *Theoret. Chim. Acta (Berlin)* **1980**, *56*, 211-230. Boudreaux, E. A.; Carsey, T. P. *Int. J. Quantum Chem.* **1980**, *18*, 469-479.

(9) Baerends, E. J.; Ellis, D. E.; Ros, P. *Chem. Phys.* **1973**, *2*, 41-51.

(10) Snijders, G. J.; Baerends, E. J.; Ros, P. *Mol. Phys.* **1979**, *38*, 1909-1929.

(11) Slater, J. C. *Adv. Quant. Chem.* **1972**, *6*, 1-92.

(12) Becke, A. J. *Chem. Phys.* **1986**, *84*, 4524-4529.

(13) Gunnarsson, O.; Lundquist, B. I. *Phys. Rev. B* **1976**, *13*, 4274-4298.

(14) Stoll, H.; Golka, E.; Preuss, H. *Theor. Chim. Acta* **1980**, *55*, 29-41.

(15) Vosko, S. H.; Wilk, L.; Nusair, M. *Can. J. Phys.* **1980**, *58*, 1200-1211.

(16) (a) Snijders, J. G.; Vernoolijs, P.; Baerends, E. J. *At. Data Nucl. Data Tables* **1981**, *26*, 483-509. (b) Vernoolijs, P.; Snijders, G. J.; Baerends, E. J. *Slater Type Basis Functions for the Whole Periodic System*; Internal Report, Free University, Amsterdam, The Netherlands, 1981.

(17) Krljin, J.; Baerends, E. J. *Fit Functions for the HFS-Method*; Internal Report (In Dutch), Free University, Amsterdam, The Netherlands, 1984.

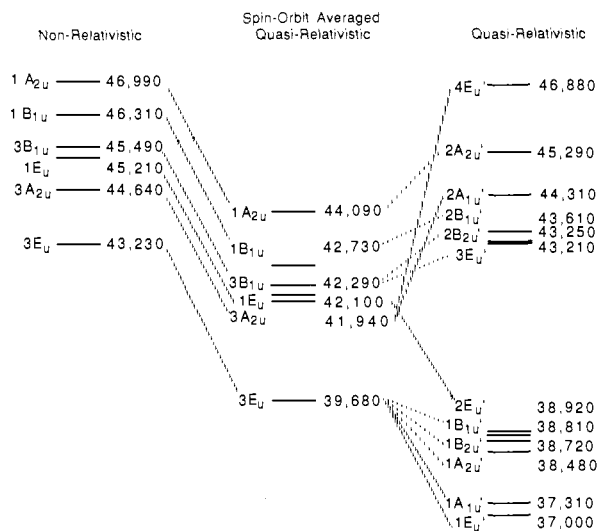


Figure 2. Energy level diagram showing the effects of relativity on the excited electronic states of $\text{Pt}(\text{CN})_4^{2-}$. The numerical values given are wavenumbers (cm^{-1}).

the exception of the $5a_{1g}$ (d_{z^2}), these orbitals all possess at least one-third ligand character. The $5a_{1g}$ is the highest occupied molecular orbital (HOMO) and consists of 91% Pt (76% $5d_{z^2}$ and 15% 6s) and 7% CN^- character.

The ordering of the d orbital energies given in Figure 1 is the same as that determined by extended Hückel calculations²³ but is different from the $d_{x^2-y^2} \gg d_{xy} > d_{xz,yz} > d_{z^2}$ ordering found from SCF- $X\alpha$ -SW calculations in both the nonrelativistic²⁴ and relativistic⁷ limits. In fact the d_{z^2} orbital is found to be 0.8 eV below the d_{xy} HOMO in the nonrelativistic calculation and 1.3 eV lower in the relativistic calculation. This discrepancy between the density functional (see the section on computational details) and SCF- $X\alpha$ -SW results is probably a result of the muffin-tin approximation used in the latter. The muffin-tin approximation represents the potential near the metal as spherical. This might be realistic for octahedral or even tetrahedral molecules but is obviously less accurate for square-planar systems. In support of this claim, we find that both the density functional and $X\alpha$ calculations give the same d-orbital energy ordering when the muffin-tin approximation is not used in the latter.

Substantial mixing between Pt 6p and $\text{CN}^- \pi^*$ orbitals is found which results in the $3a_{2u}$ orbital (43% Pt 6p, 55% $\text{CN}^- \pi^*$) being the lowest unoccupied molecular orbital (LUMO). There is negligible 6p participation in the bonding and negligible Pt 5d- $\text{CN}^- \pi^*$ backbonding. Both results are in accord with previous findings.²⁵

Also shown in Figure 1 is the influence of relativity on the one-electron energies of the d-based orbitals. As expected, the spin-orbit averaged quasi-relativistic calculation is seen to raise the energies of the d-based $5a_{1g}$, $2e_g$, and $2b_{2g}$ orbitals relative to the nonrelativistic calculation. This destabilization stems primarily from the relativistic contraction of the Pt core orbitals and the resultant increase in the shielding of the nucleus.²⁶

Spin-orbit coupling splits the $2e_g$ orbital into its $e_{1/2g}$ and $e_{3/2g}$ components by 0.36 eV. The $e_{1/2g}$ ($5a_{1g}$) and $e_{3/2g}$ ($2b_{2g}$) orbitals mix with these components to increase the splitting by an addi-

Table I. Wavenumbers and Percent Compositions of the Double Group States A_{2u}' , A_{1u}' , E_u' , and B_{2u}' for $\text{Pt}(\text{CN})_4^{2-}$ in Terms of the Corresponding Singlet and Triplet Single Group States

A_{2u}' States					
	wavenumber, cm^{-1}	$^1A_{2u}$	3E_u		
$^1A_{2u}'$	38 480	0.18	0.82		
$^2A_{2u}'$	45 290	0.82	0.18		
E_u' States					
	wavenumber, cm^{-1}	3E_u	$^3A_{2u}$	1E_u	$^3B_{1u}$
$^1E_u'$	37 000	0.56	0.39	0.03	0.02
$^2E_u'$	38 920	0.15	0.14	0.52	0.18
$^3E_u'$	43 210	0.11	0.01	0.08	0.79
$^4E_u'$	46 880	0.17	0.48	0.36	0.00
B_{1u}' States					
	wavenumber, cm^{-1}	$^1B_{1u}$	3E_u		
$^1B_{1u}'$	38 810	0.18	0.82		
$^2B_{1u}'$	43 610	0.82	0.18		
B_{2u}' States					
	wavenumber, cm^{-1}	$^3B_{1u}$	3E_u		
$^1B_{2u}'$	38 720	0.21	0.79		
$^2B_{2u}'$	43 250	0.79	0.21		
A_{1u}' States					
	wavenumber, cm^{-1}	$^3A_{2u}$	3E_u		
$^1A_{1u}'$	37 310	0.34	0.66		
$^2A_{1u}'$	44 310	0.66	0.34		

tional 0.26 eV. This causes the $e_{1/2g}$ ($2e_g$) orbital to be lower in energy than that of the $e_{3/2g}$ ($2b_{2g}$) (Figure 1). The substantial spin-orbit splitting results in the $e_{1/2g}$ HOMO having 72% $d_{\sigma}(5a_{1g})$ and 25% $d_{\pi}(2e_g)$ character. (The labels $e_{1/2}$ and $e_{3/2}$ are identical with the alternative spin-orbit labels Γ_6 and Γ_7 , respectively.)

2. $\text{Pt}(\text{CN})_4^{2-}$: Electronic Absorption Spectrum. The rich store of spectroscopic information available for **1** must be accounted for by any successful electronic structure calculation of the ion. In Figure 2 are shown the calculated wavenumbers of all the various electronic states expected to be involved in the absorption spectrum up to $50\,000\text{ cm}^{-1}$.

In comparing the nonrelativistic results to the spin-orbit averaged quasi-relativistic ones, note the uniform lowering in energy of all six states as relativistic effects are introduced. This is a simple consequence of the relativistic destabilization of the occupied $2b_{2g}$, $2e_g$, and $5a_{1g}$ orbitals compared to the unoccupied $3a_{2u}$ orbital, thereby lowering the energy gap between them (see Fig 1 and the discussion pertaining thereto). Note also in comparing the spin-orbit averaged quasi-relativistic results to the quasi-relativistic results that the range of energies involved in the transitions is more than doubled by the effects of spin-orbit splitting, which allow for the mixing of triplet and singlet states.

The percent composition of each of the spin-orbit states is given in terms of the spin-orbit averaged quasi-relativistic singlet and triplet states in Table I. The substantial coupling of the singlet and triplet states should enable all symmetry-allowed transitions to be observable.

These calculated results can be compared to the experimental data available for the absorption spectrum of **1** in the region $35\,000$ – $50\,000\text{ cm}^{-1}$ and listed in the first five columns of Table II. Taken together, the polarized single-crystal spectrum at 5 K of the $n\text{-Bu}_4\text{N}^+$ salt of **1** (column 2)²⁷ and the aqueous solution spectrum at 298 K of the same salt (column 3)²⁸ indicate the presence of as many as ten bands in this region of the absorption spectrum. Assignments of these bands based on the calculations reported here are given in the last three columns of Table II.

As can be seen, there is an excellent account given of the major bands observed (bands 1, 3, 4, 8, and 9). Bands 2 and 5 are

(23) Kasi Viswanath, A.; Krogh-Jespersen, M. B.; Vetuskey, J.; Baker, C.; Ellenson, W. D.; Patterson, H. H. *Mol. Phys.* **1981**, *42*, 1431–1451. Kasi Viswanath, A.; Vetuskey, J.; Leighton, R.; Krogh-Jespersen, M. B.; Patterson, H. H. *Mol. Phys.* **1983**, *48*, 567–579.

(24) Interrante, L. V.; Messmer, R. P. *Chem. Phys. Lett.* **1974**, *26*, 225–228. Interrante, L. V.; Messmer, R. P. In *Extended Interactions Between Metal Ions in Transition Metal Complexes*; American Chemical Society, Symposium Series; Interrante, L. V., Ed.; American Chemical Society: Washington, D.C., 1974; pp 382–391.

(25) Murgich, J.; Oja, T. J. *Chem. Soc., Dalton Trans.* **1987**, 1637–1640. Larsson, R.; Folkesson, B. *Chem. Scr.* **1982**, *19*, 31–38. Louwen, J. N.; Hengelmolen, R.; Grove, D. M.; Oskam, A.; DeKock, R. L. *Organometallics* **1984**, *3*, 908–918.

(26) Pyykkö, P. *Chem. Rev.* **1988**, *88*, 563–594.

(27) Cowman, C. D.; Gray, H. B. *Inorg. Chem.* **1976**, *15*, 2823–2824.

(28) Marsh, D. G.; Miller, J. S. *Inorg. Chem.* **1976**, *15*, 720–722. Miller, J. S.; Marsh, D. G. *Inorg. Chem.* **1976**, *15*, 2293–2295.

Table II. Spectroscopic Assignments for the Absorption Spectrum of the $\text{Pt}(\text{CN})_4^{2-}$ Ion

band	exptl wavenumber, cm^{-1}		polarization	int	orbital trans	state trans ^b A_{1g}' ($^1A_{1g}$) to	calcd wavenumber, cm^{-1}
	ref 27	ref 28					
1	35 520	35 790	xy	weak	$2e_{1g} \rightarrow 3a_{2u}$	$1E_u'$ ($^3E_u, ^1E_u$)	37 000
2		37 400 sh ^a		very weak	$2e_{1g} \rightarrow 3a_{2u}$	$1B_{1u}'$ ($^3E_u, ^1B_{1u}$) (or $1E_u' + \nu_{\text{CN}}$)	38 810
3	38 020	38 740	z	strong	$2e_{1g} \rightarrow 3a_{2u}$	$1A_{2u}'$ ($^3E_u, ^1A_{2u}$)	38 480
4	38 880	39 600	xy	strong	$2e_{1g} \rightarrow 3a_{2u}$	$2E_u'$ (1E_u)	38 920
5	39 140		z	moderate	$2e_{1g} \rightarrow 3a_{2u}$	vibronic component of $1A_{2u}'$	
6	41 070	40 970	xy,z	weak	$2b_{2g} \rightarrow 3a_{2u}$	$3E_u'$ ($^3B_{1u}, ^1E_u$)	43 210
7	44 350	43 500 sh	z,xy	weak	$2b_{2g} \rightarrow 3a_{2u}$	$2B_{1u}'$ ($^1B_{1u}$)	43 600
8	45 290	46 130	z	very strong	$5a_{1g} \rightarrow 3a_{2u}$	$2A_{2u}'$ ($^1A_{2u}$)	45 290
9	45 700	46 760	xy	strong	$5a_{1g} \rightarrow 3a_{2u}$	$4E_u'$ ($^3A_{2u}, ^1E_u$)	46 880
10		50 400		weak	$4a_{1g} \rightarrow 3a_{2u}$	c	[$\approx 53\ 000$] ^c

^ash: shoulder. ^bThe double group prime notation is used; states in parentheses refer to the dominant triplet and singlet parentages (see Table I). ^cNo state energies were calculated for this orbital transition, and so the value listed in brackets in column 8 refers to the one-electron orbital energy difference.

possibly vibronically allowed components of bands 1 and 3, respectively, although the symmetry- and spin-forbidden transition to $1A_{1g}'$ calculated to lie at $37\ 300\ \text{cm}^{-1}$ is another possibility for band 2. The suggestion that band 5 represents a component of a vibronically allowed transition has been made previously.²⁷ Band 6 is assigned to the transition to $3E_u'$, although $2E_u' + \nu_{\text{CN}}$ might also be present in this region as suggested previously.²⁹ Band 7 is assigned to the symmetry-forbidden transition to $2B_{1u}'$, which has a large amount of singlet character (see Table I). Finally, band 10 is assigned to the $4a_{1g}$ to $3a_{2u}$ orbital transition and hence would involve some ligand-to-metal charge-transfer character since the $4a_{1g}$ orbital is largely $\sigma\ \text{CN}^-$ in nature.

How do these assignments agree with previous interpretations? The ordering of the state energies neglecting spin-orbit coupling has generally been taken to be $^3A_{2u} < ^3E_u < ^1A_{2u} < ^3B_{1u} < ^1E_u < ^1B_{1u}$,²⁷⁻³⁰ substantially different than calculated here. This ordering has enabled a reasonably effective accounting to be made of the observed spectrum when spin-orbit effects have been included.²⁷⁻³⁰ However, a recent examination of the effects of solution association of **1** on its UV absorption spectrum has indicated a reversal of the ordering of the $^3A_{2u}$ and 3E_u states.³¹ This is the same ordering determined by the spin-orbit averaged quasi-relativistic density functional calculations and presented in Figure 2. The assignments given in Table II are thus consistent with this finding and are at least as successful as the alternatives²⁷⁻³¹ in accounting for the entire set of 10 bands in the UV spectrum.

The ability to account for the absorption spectrum of **1** by assuming $^3A_{2u} < ^3E_u$ in energy has been taken as evidence that the d_{z^2} -based $5a_{1g}$ orbital lies higher in energy than the $d_{xz,yz}$ -based $2e_g$ orbital.²⁷⁻³⁰ This is the same orbital energy ordering as determined by density functional calculations and presented in Figure 1. However, the ordering of the two lowest states is calculated to be $^3E_u < ^3A_{2u}$ and not the other way around. This is a simple consequence of the fact that there will be less electron-electron repulsion if, in the excited state, the unpaired electron residing in a d orbital is as far away from the unpaired electron in the $3a_{2u}$ orbital as possible. Since the $3a_{2u}$ orbital has a substantial amount of $6p_z$ character, the other unpaired electron will prefer to be in either the $2b_{2g}$ (d_{xy}) or $2e_g$ ($d_{xz,yz}$) orbitals instead of the $5a_{1g}$ (d_{z^2}) orbital to minimize interactions. This finding highlights the difficulties in determining relative orbital energies from spectroscopic state energies. A successful electronic structure calculation is thus valuable in determining such orderings.

This reversal of state energies has important consequences for other molecules as well. For example, it has been noted that the absorption spectra of $\text{Pt}(\text{NH}_3)_4^{2+}$ and **1** are very similar, and on this basis assignments for $\text{Pt}(\text{NH}_3)_4^{2+}$ analogous to those of **1** have

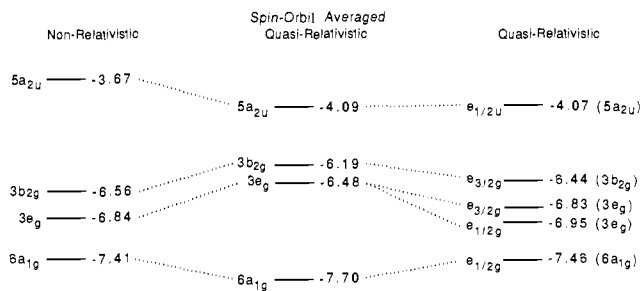


Figure 3. Orbital energy diagram showing the effects of relativity on the ordering of the Pt 5d-based orbitals in $\text{Pt}(\text{CN})_4$.

been made.³² A reconsideration of these assignments would appear to be warranted on the basis of the above findings.

Finally, there has been some discussion recently concerning the relationship between the low-energy absorption bands in columnar compounds of **1** such as $\text{Ba}[\text{Pt}(\text{CN})_4] \cdot 4\text{H}_2\text{O}$ and the absorption bands in the isolated ion.^{1,33} In particular if, as is generally accepted, the low-energy band seen in columnar compounds of **1** results from a spin- and symmetry-allowed a_{1g} ($\text{Pt}\ 5d_{z^2}$) to a_{2u} ($\text{Pt}\ 6p_z + \text{CN}^- \pi^*$) transition,^{1,34} then there should be a relationship to the corresponding transition(s) in **1**. As Tables I and II show, there are two transitions, bands 3 and 8 predicted to have substantial $^1A_{2u}$ ($5a_{1g}$ to $3a_{2u}$) character (18% and 82%, respectively). In fact, it is just these two bands that lose intensity upon association of **1**, both in concentrated aqueous solution and in columnar solids.

We differ slightly from a previous interpretation²⁸ of this observation in reversing the assignments of bands 4 and 9. Thus the decrease in the intensity of the absorption in the $37\ 000$ – $40\ 000\ \text{cm}^{-1}$ region (see Figure 3 of ref 31) can be attributed to the presence of the spin-orbit contribution of $^1A_{2u}$ to band 3 rather than a $^3A_{2u}$ component. Note that the observed intensity of band 3 suggests the amount of $^1A_{2u}$ character in this band is probably even greater than the 18% calculated.

There have been differing suggestions that the isolated ion absorption band of **1** responsible for the low-energy absorption band in its columnar compounds can be attributed either to band 3³³ or to band 8.^{1,35} Since both bands are calculated to have appreciable $^1A_{2u}$ character, both proposals seem to have merit. However, assuming the calculated ordering of the non-spin-orbit split states is correct, band 8 should have a higher amount of $^1A_{2u}$ character than band 3, even if the calculated ratio of 82% to 18% is somewhat too high.

3. $\text{Ti}_2\text{Pt}(\text{CN})_4^{2-}$. As proposed earlier³ on the basis of qualitative considerations the covalent part of the bonding between Ti and Pt in **2** is found to be largely a σ interaction involving primarily the empty $6p_z$ and filled $6s$ orbitals on the two Ti^+ ions and the

(29) Iscl, H.; Mason, W. R. *Inorg. Chem.* **1975**, *14*, 905–912. Iscl, H.; Mason, W. R. *Inorg. Chem.* **1975**, *14*, 913–918.

(30) Plepho, S. B.; Schatz, P. N.; McCafferty, A. J. *J. Am. Chem. Soc.* **1982**, *104*, 3596–3600.

(31) Schindler, J. W.; Fukuda, R. C.; Adamson, A. W. *J. Am. Chem. Soc.* **1982**, *104*, 3596–3600.

(32) Mason, W. R. *Inorg. Chem.* **1986**, *25*, 2925–2929.

(33) Musselman, R. L.; Anex, B. G. *J. Phys. Chem.* **1987**, *91*, 4460–4463.

(34) Tuszyński, W.; Glemann, G. *Ber. Bunsenges. Phys. Chem.* **1985**, *89*, 940–948.

(35) Day, P. *J. Am. Chem. Soc.* **1975**, *97*, 1588–1599.

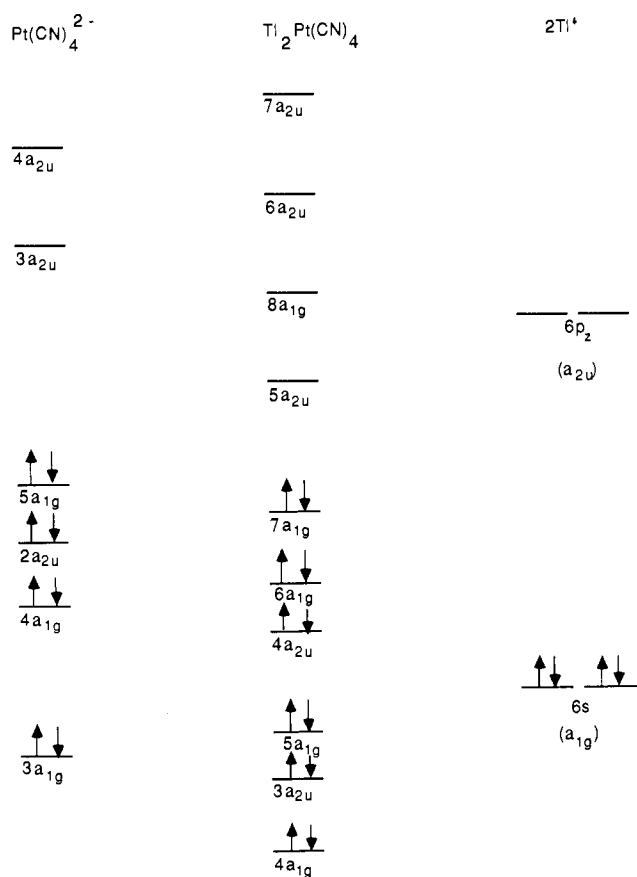


Figure 4. Orbital correlation diagram for $\text{Tl}_2\text{Pt}(\text{CN})_4$ showing the dominant $\text{Tl}^+\text{-Pt}(\text{CN})_4^{2-}$ σ interactions leading to covalency in $\text{Tl}_2\text{Pt}(\text{CN})_4$.

empty $6p_z$ ($3a_{2u}$) and filled $5d_{z^2}$ ($5a_{1g}$) orbitals on **1**. However, the $3a_{2u}$ orbital is mostly of $\text{CN}^- \pi^*$ character, and the presence of additional a_{1g} and a_{2u} orbitals (both almost completely CN^- in character) results in a somewhat more complicated picture as shown in Figures 3 and 4.

The highest occupied a_{1g} ($7a_{1g}$) orbital is found to be mostly $\text{CN}^- \sigma$ and Pt $5d_{z^2}$ in nature. Even this orbital is stabilized relative to the occupied a_{1g} orbitals in **1** through mixing with the relatively low-energy, unoccupied $6p_z$ orbitals on the Tl^+ ions. Such stabilization changes the relative ordering of the Pt $5d$ orbitals in **2** compared to **1** as shown in Figure 3. As in **1**, note the destabilization of the $3b_{2g}$ and $3e_g$ orbitals due to relativistic effects. The small relativistic stabilization of the $6a_{1g}$ (d_{z^2}) orbital is due to the presence of substantial Pt $6s$ and Tl $6p_z$ character.

The total stabilization energy E of **2** relative to 2Tl^+ and **1** was found to be 1418 kJ mol^{-1} by the density functional calculations. This stabilization energy can be decomposed into electrostatic and covalent contributions, and the latter can be decomposed further according to the contributions made by orbitals of different symmetries.³⁶ Such an analysis can be expressed by the equation

$$E = E_{\text{el}} + E_{\text{exp}} + E(a_{1g}) + E(a_{2u}) + E_{\text{ao}}$$

where E_{el} ($=1229 \text{ kJ mol}^{-1}$) is the electronic attractive energy between 2Tl^+ and **1** and E_{exp} ($=-195 \text{ kJ mol}^{-1}$) is the covalent destabilization energy resulting from two-orbital, four-electron exchange repulsion terms between occupied orbitals. $E(a_{1g})$ ($=192 \text{ kJ mol}^{-1}$), $E(a_{2u})$ ($=128 \text{ kJ mol}^{-1}$), and E_{ao} ($=64 \text{ kJ mol}^{-1}$) are the covalent energy stabilization terms for the a_{1g} , a_{2u} , and all other

symmetry orbitals, respectively. Thus the net covalent contribution (189 kJ mol^{-1}) to the bonding is only 13% of the total stabilization energy.

The prediction made earlier that the absorption band of **2** centered at 27000 cm^{-1} is due to an a_{1g} to a_{2u} transition³ is shown to be only partially correct. Although the LUMO is found to be an a_{2u} orbital of largely $\text{Tl}^+ 6p_z$ character ($5a_{2u}$), the lowest spin- and symmetry-allowed transition is predicted to be $3b_{2g}$ to $5a_{2u}$ (19100 cm^{-1} based on one-electron orbital energy differences). Other allowed transitions predicted to lie within 10000 cm^{-1} (the width of the lowest energy band observed in the absorption spectrum of **2**) of this value include the $3e_g$ to $5a_{2u}$ and $6a_{1g}$ to $5a_{2u}$ transitions and several CN^- to Tl^+ charge-transfer transitions involving not only the $5a_{2u}$ orbital but the empty $6p_{x,z}$ Tl^+ orbitals ($7e_u$ and $4e_g$) as well. Thus the presence of Tl^+ in the molecule provides a spectroscopic probe that enables states derived from the Pt $5d_{xy}$ and $5d_{xz}, d_{yz}$ orbitals to be directly observed. Clearly a polarized single-crystal absorption study at low temperatures would be useful in testing this prediction. Since calculations of the various excited electronic states involved have not been carried out, it is not possible at this time to predict which state is responsible for the observed luminescence centered at 22500 cm^{-1} .³

The calculations show further that the covalent contribution to the bonding is largely the result of a synergistic interaction between the Tl^+ ions and **1** in which the empty $6p_z$ orbitals of Tl^+ accept electron density from **1** and the filled $6s$ orbitals donate electron density to **1** in a balanced way. Both a_{1g} and a_{2u} orbitals are involved in this process, and no attempt was made to decompose the relative contributions of each type of orbital. The relatively low-energy absorption band of **2** is seen from Figure 4 to result directly from this interaction as predicted earlier.³ Although all other metal ions, including Pb^{2+} ,³⁷ that form solid compounds with **1** result in columnar stacking,² the ability of **1** and the Tl^+ ions to form a small but substantial covalent interaction apparently interferes with the stacking process. This suggests, as expected, a relatively weak covalent interaction among the Pt atoms in unoxidized columnar solids of **1**.

Conclusions

The density functional calculations on **1** have helped to clarify many of the unresolved issues regarding the spectroscopic properties of **1**. In particular a satisfactory resolution between the ordering of the Pt $5d$ orbital energies and the spectroscopic transition energies has been achieved. The inclusion of relativistic effects, especially spin-orbit coupling, has been shown to be crucial in making accurate spectroscopic assignments.

The calculations on **2** indicate the Pt-Tl bonding involves primarily electrostatic forces, but a significant covalent interaction (189 kJ mol^{-1}) is also present. As had been predicted earlier on the basis of qualitative considerations³ this covalent interaction has been shown to involve substantial σ orbital overlap between the $6s$ and $6p_z$ valence orbitals of Tl and the $5d_{z^2}$ and $6p_z$ valence orbitals of Pt. In addition, however, the calculations reveal that both the filled σ and empty π orbitals of CN^- also play an important role in the interaction. Furthermore the influence of relativistic effects in the bonding between heavy metal atoms such as Tl and Pt^{3,4d,e,26} is clearly demonstrated by these calculations.

Acknowledgment. Financial assistance provided by the Faculty Research Committee of Bowdoin College to support the visit of J.K.N. to the University of Calgary is gratefully acknowledged. This investigation was supported by the Natural Sciences and Engineering Research Council of Canada. We thank also the University of Calgary for access to its Cyber-205 installations.

(36) Ziegler, T.; Rauk, A. *Inorg. Chem.* **1979**, *18*, 1558-1565.

(37) Nagle, J. K.; Balch, A. L.; Olmstead, M. M., unpublished results.